



# HHS Public Access

Author manuscript

*Eur J Med Chem.* Author manuscript; available in PMC 2024 May 05.

Published in final edited form as:

*Eur J Med Chem.* 2023 May 05; 251: 115246. doi:10.1016/j.ejmech.2023.115246.

## From PROTAC to inhibitor: Structure-guided discovery of potent and orally bioavailable BET inhibitors

Mladen Koravovic<sup>a,§</sup>, Anand Mayasundari<sup>b,§</sup>, Gordana Tasic<sup>a</sup>, Fatemeh Keramatnia<sup>b</sup>, Timothy R Stachowski<sup>b</sup>, Huarui Cui<sup>c</sup>, Sergio C Chai<sup>b</sup>, Barbara Jonchere<sup>d</sup>, Lei Yang<sup>b</sup>, Yong Li<sup>b</sup>, Xiang Fu<sup>b</sup>, Ryan Hiltenbrand<sup>e</sup>, Leena Paul<sup>f</sup>, Vibhor Mishra<sup>g</sup>, Jeffery M. Klco<sup>e</sup>, Martine F. Roussel<sup>d</sup>, William CK Pomerantz<sup>c</sup>, Marcus Fischer<sup>b</sup>, Zoran Rankovic<sup>b,\*</sup>, Vladimir Savic<sup>a,\*</sup>

<sup>a</sup>University of Belgrade, Faculty of Pharmacy, Department of Organic Chemistry, Vojvode Stepe 450, 11221 Belgrade, Serbia

<sup>b</sup>Department of Chemical Biology & Therapeutics, St. Jude Children's Research Hospital, 262 Danny Thomas Place, Memphis, TN 38105

<sup>c</sup>Department of Chemistry, University of Minnesota, 207 Pleasant Street SE, Minneapolis, Minnesota 55455, United States

<sup>d</sup>Department of Tumour Cell Biology, St. Jude Children's Research Hospital, 262 Danny Thomas Place, Memphis, TN 38105

<sup>e</sup>Department of Pathology, St. Jude Children's Research Hospital, 262 Danny Thomas Place, Memphis, TN 38105

<sup>f</sup>Department of Developmental Neurobiology, St. Jude Children's Research Hospital, 262 Danny Thomas Place, Memphis, TN 38105

<sup>g</sup>Department of Pathology, St. Jude Children's Research Hospital, 262 Danny Thomas Place, Memphis, TN 38105

### Abstract

\*Corresponding authors; ZR: zoran.rankovic@stjude.org, VS: vladimir.savic@pharmacy.bg.ac.rs.

§Contributed equally to this work

Author contributions:

MK, synthesis, data collection and analysis, manuscript writing and revision. AM, synthesis, study design and coordination, data collection and analysis, manuscript writing and revision. GT, synthesis, data analysis, manuscript revision, FK, data collection and analysis. TRS, structural biology, manuscript writing and revision. HC, provided reagents. LY, data collection and analysis. YL, data collection and analysis. XF, data collection and analysis. SC, data collection and analysis. BJ, data collection. RH, data collection. LP, data collection and analysis. VM, data collection and analysis. WCKP, provided reagents. MFR, supervision, medulloblastoma cell lines data generation and analysis, manuscript writing and revision. JMK, supervision, ALL cell lines data generation and analysis, manuscript writing and revision. MF, supervision, data analysis, structural biology, manuscript writing and revision. ZR, conceived the study, supervision, data analysis, manuscript writing and revision. VS, supervision, data analysis, manuscript writing and revision

Declaration of interests

The authors declare that they have no known competing financial interests or personal relationships that could have appeared to influence the work reported in this paper.

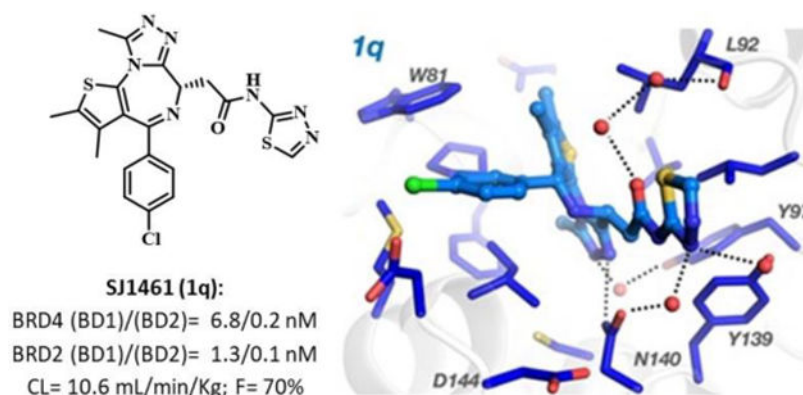
Supporting Information

The Supporting Information, experimental procedures and spectral data, is available.

**Publisher's Disclaimer:** This is a PDF file of an unedited manuscript that has been accepted for publication. As a service to our customers we are providing this early version of the manuscript. The manuscript will undergo copyediting, typesetting, and review of the resulting proof before it is published in its final form. Please note that during the production process errors may be discovered which could affect the content, and all legal disclaimers that apply to the journal pertain.

An X-ray structure of a CLICK chemistry-based BET PROTAC bound to BRD2(BD2) inspired synthesis of JQ1 derived heterocyclic amides. This effort led to the discovery of potent BET inhibitors displaying overall improved profiles when compared to JQ1 and birabresib. A thiaziazole derived **1q** (SJ1461) displayed excellent BRD4 and BRD2 affinity and high potency in the panel of acute leukaemia and medulloblastoma cell lines. A structure of **1q** co-crystalised with BRD4-BD1 revealed polar interactions with the AZ/BC loops, in particular with Asn140 and Tyr139, rationalising the observed affinity improvements. In addition, exploration of pharmacokinetic properties of this class of compounds suggest that the heterocyclic amide moiety improves drug-like features. Our study led to the discovery of potent and orally bioavailable BET inhibitor **1q** (SJ1461) as a promising candidate for further development.

## Graphical Abstract



## Keywords

BET inhibitors; JQ1; amides

## Introduction

Histones are positively charged proteins that enable cells to pack and protect DNA molecules via interactions of lysine residues with acidic phosphate moieties of DNA creating chromatin.[1] [2] Stability of this complex can be affected by acetylation of the  $\epsilon$ -amino functionality of lysine, a transformation that eliminates basicity of this group and prevents its involvement in the ionic bond formation with the phosphates.[3] [4] [5] A consequence of the acetylation is a loss of DNA-histone contacts and formation of a complex with weak interactions which consequently promotes gene expression. One of the major mechanisms of chromatin activation involves recognition of N-acetyl lysine residue at the N-terminal tails of histones by the Bromo- and Extra-Terminal domain (BET) family of proteins. [6] [7] [8] Four members of this family have been described to date: BRD2, BRD3, BRD4 and BRDT. [9] [10] [11] [12] [13] [14] The structure of BET proteins comprises of two bromodomains (BD1 and BD2), an extraterminal domain (ET) and a C-terminal domain (CTD). [15] The BDs are hydrophobic regions created by four  $\alpha$ -helices (Z, A, B and C) and two loops (ZA and BC) and can recognise N-acetyl residue in histones and other proteins. [16] The ET domain is involved in recruitment of various components

of the transcriptional complexes while CTD, present only in BRD4 and BRDT, interact with positive elongation factor (p-TEFb). [17] [18] BET proteins are involved in various pathophysiological processes, but particularly important is their role in cancer development. [19] [20] [21] In recent years a range of BET inhibitors have been described in the literature (Figure 1). [22] [23] [24] [25]

The first amongst them was diazepine derivative **1a** known as JQ1, now widely used as a tool in studying BET biology. [26] JQ1 displaces BRD4 from chromatin and induces differentiation, G1 cell cycle arrest and apoptosis in cancer cells such as human-derived NUT midline carcinoma. [27] However, the compound's short half-life in vivo prevented its progression into clinical studies. [28] On the other hand, its amide derivative known as birabresib, **1c**, entered clinical trial demonstrating dose-proportional exposure, favourable safety profile and activity in NMC. [29] Our interest in BET inhibitors sparked from an X-ray structure of a CLICK chemistry-based BET PROTAC bound to BRD2(BD2) revealing novel ligand-protein interactions. This observation followed by an optimization effort described here led to the discovery of potent BET inhibitors displaying overall improved profiles when compared to JQ1 and birabresib.

## 2. Results and discussion

### 2.1. Background of the study

Proteolysis-targeting chimeras (PROTACs) have received considerable attention in recent years as a promising novel paradigm in drug discovery. [30] [31] [32] [33] [34] [35] [36] [37] [38] Our interest in developing novel BET-PROTACs led us to the discovery of a series of CLICK-based degraders such as **7** that displayed significantly increased affinity in BRD2 TR-FRET assay compared to parent JQ1 **1a** and related PROTACs such as dBET1 **8**. [39] [40] [41]

This finding suggests that the side chain of the click PROTAC forms additional interactions resulting in improved BRD affinity. Indeed, the crystal structure of CLICK-PROTAC **7** in complex with BRD2/BD2 that we previously generated (PDB: 6WWB) showed several additional interactions with the protein compared to JQ1, which included a water-bridged hydrogen bond network between NH-amide/Asn429 and CO-amide/Leu381, and hydrogen bonding between the amide triazole/His433 (Figure 3A). [39] The electron density around the thalidomide part of ligand **7** was weak and its role is not clear. The crystal structure generally revealed that the network of H-bonds created by **7** is similar to **1a** (JQ1) in the corresponding region except JQ1 is lacking an interaction with Leu381 (Figure 3B) (PDB:3ONI). [26] Similarly to **1a**, **1c** (birabresib) in complex with related BRD4 (PDB: 5WMD) adopts an analogous conformation with the key interactions involving the amide functionality (Figure 3C). [42] Here the H-bonding network is more complex and includes water-mediated H-bonds with Leu92, Asn140, and with a non-conserved Asp144 in lieu of His433 in BRD2. The phenol moiety of **1c** that is projecting towards the solvent may be important for balancing other properties of this ligand. All three ligands maintain H-bonding with the conserved Tyr386 via a water molecule. These results suggest the critical role of the triazole moiety in improving the affinity of the PROTAC ligand towards BRD2/BD2.

## 2.2. Chemistry

To explore and further leverage these novel interactions, we synthesised several JQ1 amide derivatives and compared their properties with the parent inhibitor as well as with a more potent birabresib **1c** (Table 1). Our focus was on substituents that can probe the subpocket occupied by the 1,2,3-triazole in **7**. Consequently, majority of compounds contained heterocyclic substituents with the potential to create H-bonding interactions. All amides were synthesised from the appropriate acid **9** and amine using either HATU or DEPBT as coupling reagent in presence of DIPEA as base and in DMF as solvent, Scheme 1. The amides were isolated by column chromatography in 20–95% yields.

## 2.3. BRD2/BRD4 binding assay

Binding affinity of the synthesised amides were determined in TR-FRET assay against BRD4 and BRD2 proteins, as shown in Table 1. For both proteins BD2 seems to be more sensitive towards the ligands with several compounds showing sub-nanomolar activity and better potency than JQ1 **1a** or birabresib **1c**. In general, majority of compounds possessing a heterocyclic ring within the amide moiety showed higher affinity to BRD2 than the parent JQ1 **1a** or birabresib **1c**. Interestingly, glycine ester derivative **1m** (IC<sub>50</sub> BRD2/BD1 3.4nM), also showed a high affinity in this assay, possibly having the ester group engaged with the protein in a similar, bioisosteric fashion to five membered heterocycles. [43] [44] This is well exemplified by comparing the activities of **1m** (IC<sub>50</sub> BRD2/BD1 3.4nM) and oxazole derivative **1i** (IC<sub>50</sub> BRD2/BD1 9.2nM). Derivatives with the benzyl type of structure, **1d-f**, **1h**, **1i** and **1k**, were less potent than the most active thiadiazole **1q** (IC<sub>50</sub> BRD2/BD1 1.6nM) with the shorter amide chain. Notably, structurally similar to **1q**, thiazole derivative **1o** (IC<sub>50</sub> BRD2/BD1 10.9nM) demonstrated lower affinity suggesting significance of an additional nitrogen or perhaps better positioning for the H-bonding interacting group. Surprisingly, we did not observe a difference between **1k** (IC<sub>50</sub> BRD2/BD1 16.3nM) and the N-deleted analogue **1g** (IC<sub>50</sub> BRD2/BD1 21.7nM). This may suggest that positioning of heteroatom in the amide moiety is important for the affinity. A similar trend was observed in the BRD4 assay. Derivative **1q** (IC<sub>50</sub> BRD4/BD1 6.5nM) was amongst the most active compounds with isoxazole **1h** (IC<sub>50</sub> BRD4/BD1 5.7nM) having comparable activity and glycine derivative **1m** (IC<sub>50</sub> BRD4/BD1 2.8nM) being even slightly more potent.

Overall, several of our most active compounds described above performed better in both BRD4 and BRD2 binding assays than JQ1 **1a** or birabresib **1c** (Table 1).

## 2.4. Cell-based assay

Encouraging initial results prompted further profiling of the synthesised amides in cancer cell viability assays. The cell line selection was influenced by our general focus on high risk paediatric cancers such as acute leukaemia (MV4–11, NALM-16, MOLM-13) and medulloblastoma (HDMB03, D283), the two leading causes of childhood cancer death. (Table 2). Cells were treated with compounds over 72 hours, and their viability was assessed using the CellTiter-Glo assay kit (Promega). The IC<sub>50</sub> values were determined by the proprietary software Robust Investigation of Screening Experiments (RISE), developed in house on the Pipeline Pilot platform (Biovia, v. 17.2.0). [45] Medulloblastoma cells

HDMB03 showed high sensitivity towards **1i** (IC<sub>50</sub> 1.0nM) and **1q** (IC<sub>50</sub> 6.6nM), which were very potent in biochemical assays as well. Compound **1i** was ~90-fold and ~130-fold more toxic than JQ1 **1a** (IC<sub>50</sub> 90.3nM) and birabresib **1c** (IC<sub>50</sub> 134.3.3nM), respectively. It is also worth noting that heterocyclic amides **1o** (IC<sub>50</sub> 4.6nM) and **1d** (IC<sub>50</sub> 3.8nM) showed >20-fold better potency than **1a** or **1c**. Leukaemia cells NALM16 displayed similar sensitivity towards **1i** (IC<sub>50</sub> 0.8nM) and **1q** (IC<sub>50</sub> 3.6nM), while birabresib **1c** (IC<sub>50</sub> 14.0nM) demonstrated ~15-fold lower potency than **1i**. Additional heterocyclic amides such as **1d** (IC<sub>50</sub> 7.3nM) or **1o** (IC<sub>50</sub> 6.4nM) also showed significant potency against this cell line supporting generally observed trend for the JQ1 heterocyclic amide derivatives. A similar tendency was observed in other cell lines, although, with less significant differences in activity of the most active amides **1i/1q** and JQ1 **1a**/birabresib **1c** (Table 2). Glycine derivative **1m** showed differences between the results obtained in two assay formats. Specifically, **1m** showed considerably higher affinity in TR-FRET assay (IC<sub>50</sub> BRD2/BD1 3.4nM, IC<sub>50</sub> BRD4/BD1 2.8nM) compared to its activity in cell-based assays (IC<sub>50</sub> 9.9–359.2nM). Similar trends were obtained with other two amino acid amide analogues **1l** and **1j**. The observed lower potency in the cell-based assays might indicate susceptibility of the amino acid derive amides to hydrolytic transformations affecting activity of these compounds.

Based on overall properties compound **1q** was selected as a lead compound and progressed to BROMOscan™ profiling, where it showed high affinity for all BET isoforms (Figure S2). Furthermore, the lead compound **1q** effect on MYC was assessed in MV4–11 cell line by immunoblotting. In this study **1q** showed a very similar profile to JQ1 and birabresib. After 6 hours incubation at 100 nM concentration of **1q** MYC protein abundance were reduced to around 50%, while at 1 μM concentration of **1q** MYC protein levels were down to 22% (Figure S3/4).

## 2.5. Structural studies

Given the promising activity of JQ-derived heterocyclic amide analogues we set to explore interactions of these derivatives with BRD proteins in more detail. We solved the X-ray crystal structures of two of our compounds, **1k** and **1q**, bound to BRD4/BD1 (Figure 4a–b). At resolutions of 1.05 Å with **1k** (PDB: 7RN2) and 1.18 Å with **1q** (PDB: 7RMD) the electron density for placement of the ligand is unambiguous (Figure S5). Analysis of the binding mode shows that both **1k** and **1q** occupy the same position in the active site of BRD4/BD1 as JQ1 **1a** and birabresib **1c**, Figure 4c–d. In all cases, the conserved diazepine fragment is located deep in the pocket and H-bonds with Tyr97 through a water molecule. The amide substituents, pyridine in **1k** and thiadiazole in **1q**, are oriented in the same area of the binding pocket as the ester moiety in JQ1 **1a** or the amide fragment of birabresib **1c** and interact with ZA and BC loop residues. Like **1a/1c**, **1k** and **1q** H-bond directly with the amide NH moiety of Asn140 in the BC loop. Although **1k** and **1q** both contain a triazole functionality, the amide substituents are oriented orthogonally to one another and thus interact with the CO moiety of Asn140 in different ways. The conserved water bridging the H-bond with Asn140-CO binds to the secondary amide in **1k** but interacts with the thiadiazole nitrogen of **1q**. This allows the pyridine nitrogen of **1k** to interact with a second water creating an additional H-bond with Asn140-CO like in JQ1 **1a** and birabresib **1c**. This

second water-mediated H-bond involves Asp144 as well, which **1q** lacks. Yet, **1q** contains a unique interaction where the thiadiazole interacts with Tyr139 in the BC loop, again through a water-mediated H-bond. Another water-mediated H-bond bridges the amide carbonyl in **1k** to the backbone oxygen of Leu92 in the ZA loop and is also observed in birabresib **1c**. This interaction requires two waters in **1q** and is missing in JQ1 **1a**. The variability in water placement between **1q**, **1a**, and **1c/1k** is most likely a consequence of the orientation of the analogues. This suggests that the amide group is critical for high affinity but also demonstrates that additional important H-bonding interactions are possible by the amide substituent. It is also worth noting that all these additional contacts are created on the rim of the BD binding pocket towards the solvent. Therefore, this provides opportunity to further derivatise the amide moiety to optimise, for example, physico-chemical properties without diminishing binding affinity.

## 2.6. Physico-chemical and ADME studies

Upon demonstrating the beneficial effect of the heterocyclic substituent for the anti-tumour cell activity of JQ1 derivatives, we sought to determine how this moiety influences their drug-like properties (Table 3, and Supporting Information). [46] Solubility for the compounds was established in phosphate buffer solution after 18h incubation period at room temperature (Table 3). [47] Concentration of dissolved compounds was measured by UV spectrometry. The solubility of heterocyclic amides was found to be generally greater than that of JQ1 **1a** (37.5 $\mu$ M) or birabresib **1c** (23.4 $\mu$ M), with triazole **1e** (80.8 $\mu$ M) being the most soluble. The solubility of pyridine derivative **1k** (72.5 $\mu$ M), was comparable to **1e**, whereas thiadiazole derivative **1q** (12.0 $\mu$ M), showed lower solubility than its derivatives, including JQ1 **1a** and birabresib **1c**. Next, we evaluated permeability of the amides using parallel artificial membrane permeability (PAMPA) and Caco2 assays. [48] [49] PAMPA assay was performed in parallel with compounds dissolved in DMSO and further diluted with phosphate buffer solutions. Donor and acceptor plates were analysed by UV spectrometry after incubation period of 0.5h. The results outlined in Table 3 suggested that the presence of polar NH/OH bond slowed down permeation of compounds (**1d**, 2.1; **1n** 20,8; **1j**, 0; **1l**,  $0.5 \times 10^{-6}$ cm/s) through the nonpolar PAMPA membrane while the heterocycle ring seemed to have a balanced effect. Lead compound **1q** ( $534.0 \times 10^{-6}$ cm/s) demonstrated good permeability, while the compounds with lipophilic amide groups showed the highest permeation (**1a** >1800, **1g** 1797.1; **1p** >1800  $\times 10^{-6}$ cm/s). In Caco2 assay we observed low permeability for the above mentioned NH/OH derivatives while **1h** ( $P_{app}$  150.34nm/s), **1k** ( $P_{app}$  98.4 nm/s) and **1q** ( $P_{app}$  66.5 $\times$  nm/s) performed better than others. Compared to the heterocyclic amides birabresib **1c** ( $P_{app}$  221.6 nm/s) showed better permeability in Caco 2 than PAMPA assay. Interestingly, whereas some of the analogues such as **1f** and **1e** were subjects of a high efflux, lead compound **1q** displayed low efflux ratio in the Caco2 assay.

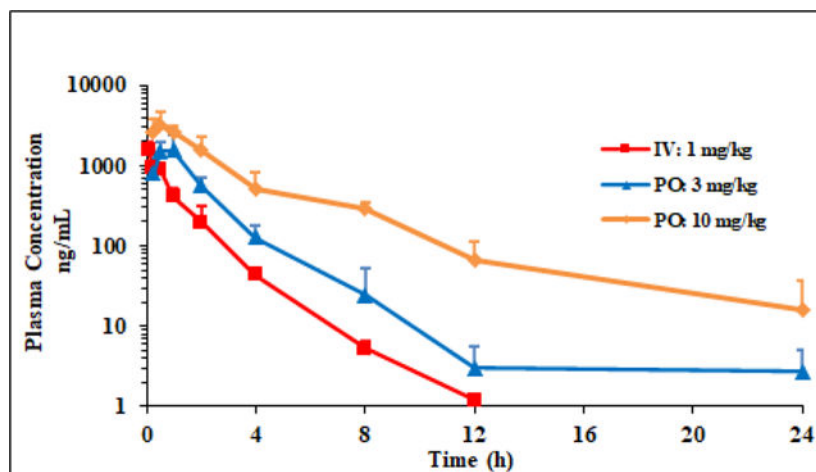
Plasma protein binding of a drug or a studied compound is important pharmacokinetic parameter as it can be often related to their efficacy. [50] Lower level of protein binding makes larger proportion of the drug/compound available to reach the biological target. Our experiments to determine this factor were performed using Rapid Equilibrium Dialysis (RED) Assay (Table 3). The results suggested high level of binding for all heterocyclic



amides (>90%) including JQ1 **1a** and birabresib **1c**. With the current set of compounds, we did not observe significant changes in this parameter with variations of the heterocyclic ring. Human plasma stability experiments were performed by incubating the compounds for up to 48h followed by LC-MS/MS analysis. Majority of the compounds showed excellent stability including derivative **1q** (100%), Table 3. Finally, we investigated metabolic stability of the synthesised amides in human microsomes (Table 3). [51] Amongst the amide derivatives lead compound **1q** ( $t_{1/2}$  3.2h) showed moderate metabolic stability while pyridine derivative **1k** ( $t_{1/2}$  0.1h) and benzyl derivative **1g** ( $t_{1/2}$  0.1h) were subjects of rapid metabolic transformation. Notably, the human microsome stability of lead compound **1q** was also better than that of JQ1 **1a** ( $t_{1/2}$  0.4h) or birabresib **1c** ( $t_{1/2}$  1.7h).

## 2.7. In vivo pharmacokinetic studies

The promising overall properties of **1q** warranted its progression into *in vivo* pharmacokinetic studies. [52] This was carried out in female CD1 mice following a single intravenous (at 1mg/kg) and oral administration (at 3mg/kg and at 10mg/kg). Blood samples were collected over a time course and they were analysed by LC-MS/MS method. The critical pharmacokinetic parameters are outlined in Table 4.



Compound **1q** showed low plasma clearance ( $Cl=10.6$  mL/min/kg) and volume of distribution typical of non-basic compounds ( $V_{ss}=0.8$  L/Kg), with elimination half-life of 1.5h. Subsequent P.O. experiments performed with 3mg/kg and 10mg/kg doses suggested good absorption ( $T_{max}$  1hr and 0.5hr, respectively) and high bioavailability (Table 4).

## 3. Conclusion

A follow up on an observation from our CLICK-derived BET-PROTACs program led to the discovery of JQ1-derived amides with overall properties comparable or better to those of JQ1 and currently clinically studied birabresib. Biochemical assay demonstrated >20-fold better potency of thiaziazole derived **1q** (SJ1461) towards BRD4/BRD2, while investigation in a panel of cancer cell lines suggested particular sensitivity of HDMB03 towards oxazole **1i** (~130- fold more potent than birabresib **1c**). Initially studied pharmacokinetic parameters of the amides are comparable to those of birabresib **1c** but the drawback for **1c** is the

potentially toxicophoric *p*-aminophenol as constitutional part of its structure. Analysis of the crystal structure of BRD4(BD1)-**1q/1k** provided an insight into the protein-ligand interactions revealing novel contacts that can be exploited for improving activity of JQ1 derivatives. The heterocyclic moiety was also shown to project towards the solvent implicitly suggesting potential route to optimise physicochemical properties of the studied compounds. The overall in vitro/vivo properties of SJ1461 makes this compound promising candidate for further exploration.

## 4. Experimental

All experimental procedures are delineated in Supporting Information.

## Supplementary Material

Refer to Web version on PubMed Central for supplementary material.

## Acknowledgment

This work was supported by ALSAC and R35GM142772 (to MF), and R35GM140837 (to WCKP). Crystallographic data were collected at Southeast Regional Collaborative Access Team (SER-CAT) 22-ID beamline at the Advanced Photon Source, Argonne National Laboratory. SER-CAT is supported by its member institutions, and equipment grants (S10\_RR25528, S10\_RR028976 and S10\_OD027000) from the National Institutes of Health. Use of the Advanced Photon Source was supported by the U. S. Department of Energy, Office of Science, Office of Basic Energy Sciences, under Contract No. W-31-109-Eng-38. This research was also supported by the Science fund of the Republic of Serbia: program, Diaspora; Grant no: 6463913; Acronym DeSyHPRO and by the Ministry of Education, Science and Technological Development, Republic of Serbia, Grant Agreement with University of Belgrade-Faculty of Pharmacy No: 451-03-9/2021-14/200161.

## References

- [1]. Hnilica LS, Structure and Biological Functions of Histones, 1st edition, CRC Press, Boca Raton, 2017.
- [2]. Shen C, ed., Histones: Class, Structure and Function, 1st edition, Nova Science Pub Inc, New York, 2012.
- [3]. Lee CY, Grant PA, Chapter 1–1 - Role of Histone Acetylation and Acetyltransferases in Gene Regulation, in: McCullough SD, Dolinoy DC (Eds.), Toxicoeugenetics, Academic Press, 2019: pp. 3–30.10.1016/B978-0-12-812433-8.00001-0.
- [4]. Verdone L, Agricola E, Caserta M, Di Mauro E, Histone acetylation in gene regulation, Brief. in Func. Genomics. 5 (2006) 209–221. 10.1093/bfpg/ell028.
- [5]. Struhl K, Histone acetylation and transcriptional regulatory mechanisms, Genes Dev. 12 (1998) 599–606. [PubMed: 9499396]
- [6]. Romero FA, Taylor AM, Crawford TD, Tsui V, Cote A, Magnuson S, Disrupting Acetyl-Lysine Recognition: Progress in the Development of Bromodomain Inhibitors, J. Med. Chem. 59 (2016) 1271–1298. 10.1021/acs.jmedchem.5b01514. [PubMed: 26572217]
- [7]. Umehara T, Nakamura Y, Jang MK, Nakano K, Tanaka A, Ozato K, Padmanabhan B, Yokoyama S, Structural Basis for Acetylated Histone H4 Recognition by the Human BRD2 Bromodomain, J. Biol. Chem. 285 (2010) 7610–7618. 10.1074/jbc.M109.062422. [PubMed: 20048151]
- [8]. Mujtaba S, Zeng L, Zhou M-M, Structure and acetyl-lysine recognition of the bromodomain, Oncogene. 26 (2007) 5521–5527. 10.1038/sj.onc.1210618. [PubMed: 17694091]
- [9]. Schwalm MP, Knapp S, BET bromodomain inhibitors, Curr. Opin. Chem. Biol. 68 (2022) 102148. 10.1016/j.cbpa.2022.102148. [PubMed: 35462054]
- [10]. Stathis A, Bertoni F, BET Proteins as Targets for Anticancer Treatment, Cancer Discov. 8 (2018) 24–36. 10.1158/2159-8290.CD-17-0605. [PubMed: 29263030]



- [11]. Padmanabhan B, Mathur S, Manjula R, Tripathi S, Bromodomain and extra-terminal (BET) family proteins: New therapeutic targets in major diseases, *J. Biosci.* 41 (2016) 295–311. 10.1007/s12038-016-9600-6. [PubMed: 27240990]
- [12]. Sahai V, Redig AJ, Collier KA, Eckerdt FD, Munshi HG, Targeting BET bromodomain proteins in solid tumors, *Oncotarget.* 7 (2016) 53997–54009. 10.18632/oncotarget.9804. [PubMed: 27283767]
- [13]. Taniguchi Y, The Bromodomain and Extra-Terminal Domain (BET) Family: Functional Anatomy of BET Paralogous Proteins, *Int. J. Mol. Sci.* 17 (2016) 1849. 10.3390/ijms17111849. [PubMed: 27827996]
- [14]. Ali HA, Li Y, Bilal AHM, Qin T, Yuan Z, Zhao W, A Comprehensive Review of BET Protein Biochemistry, Physiology, and Pathological Roles, *Front. Pharmacol.* 13 (2022) article 818891. <https://www.frontiersin.org/articles/10.3389/fphar.2022.818891> [PubMed: 35401196]
- [15]. Werner MT, Wang H, Hamagami N, Hsu SC, Yano JA, Stonestrom AJ, Behera V, Zong Y, Mackay JP, Blobel GA, Comparative structure-function analysis of bromodomain and extraterminal motif (BET) proteins in a gene-complementation system, *J. Biol. Chem.* 295 (2020) 1898–1914. 10.1074/jbc.RA119.010679. [PubMed: 31792058]
- [16]. Ferri E, Petosa C, McKenna CE, Bromodomains: Structure, function and pharmacology of inhibition, *Biochem. Pharmacol.* 106 (2016) 1–18. 10.1016/j.bcp.2015.12.005. [PubMed: 26707800]
- [17]. Aiyer S, Swapna GVT, Ma L-C, Liu G, Hao J, Chalmers G, Jacobs BC, Montelione GT, Roth MJ, A common binding motif in the ET domain of BRD3 forms polymorphic structural interfaces with host and viral proteins, *Structure.* 29 (2021) 886–898.e6. 10.1016/j.str.2021.01.010. [PubMed: 33592170]
- [18]. Crowe BL, Larue RC, Yuan C, Hess S, Kvaratskhelia M, Foster MP, Structure of the Brd4 ET domain bound to a C-terminal motif from  $\gamma$ -retroviral integrases reveals a conserved mechanism of interaction, *Proc. Natl. Acad. Sci. U.S.A.* 113 (2016) 2086–2091. 10.1073/pnas.1516813113. [PubMed: 26858406]
- [19]. Shorstova T, Foulkes WD, Witcher M, Achieving clinical success with BET inhibitors as anti-cancer agents, *Br. J. Cancer.* 124 (2021) 1478–1490. 10.1038/s41416-021-01321-0. [PubMed: 33723398]
- [20]. Sarnik J, Popławski T, Tokarz P, BET Proteins as Attractive Targets for Cancer Therapeutics, *Int. J. Mol. Sci.* 22 (2021) 11102. 10.3390/ijms222011102. [PubMed: 34681760]
- [21]. Trojer P, Targeting BET Bromodomains in Cancer, *Annu. Rev. Cancer Biol.* 6 (2022) 313–336. 10.1146/annurev-cancerbio-070120-103531.
- [22]. Schwalm MP, Knapp S, BET bromodomain inhibitors, *Curr. Opin. Chem. Biol.* 68 (2022) 102148. 10.1016/j.cbpa.2022.102148. [PubMed: 35462054]
- [23]. Feng L, Wang G, Chen Y, He G, Liu B, Liu J, Chiang C-M, Ouyang L, Dual-target inhibitors of bromodomain and extra-terminal proteins in cancer: A review from medicinal chemistry perspectives, *Med. Res. Rev.* 42 (2022) 710–743. 10.1002/med.21859. [PubMed: 34633088]
- [24]. Chen J, Tang P, Wang Y, Wang J, Yang C, Li Y, Yang G, Wu F, Zhang J, Ouyang L, Targeting Bromodomain-Selective Inhibitors of BET Proteins in Drug Discovery and Development, *J. Med. Chem.* 65 (2022) 5184–5211. 10.1021/acs.jmedchem.1c01835. [PubMed: 35324195]
- [25]. Fu Y, Zhang Y, Sun H, Progress in the development of domain selective inhibitors of the bromo and extra terminal domain family (BET) proteins, *Eur. J. Med. Chem.* 226 (2021) 113853. 10.1016/j.ejmech.2021.113853. [PubMed: 34547507]
- [26]. Filippakopoulos P, Qi J, Picaud S, Shen Y, Smith WB, Fedorov O, Morse EM, Keates T, Hickman TT, Felletar I, Philpott M, Munro S, McKeown MR, Wang Y, Christie AL, West N, Cameron MJ, Schwartz B, Heightman TD, La Thangue N, French CA, Wiest O, Kung AL, Knapp S, Bradner JE, Selective inhibition of BET bromodomains, *Nature.* 468 (2010) 1067–1073. 10.1038/nature09504. [PubMed: 20871596]
- [27]. Jiang G, Deng W, Liu Y, Wang C, General mechanism of JQ1 in inhibiting various types of cancer, *Mol. Med. Rep.* 21 (2020) 1021–1034. 10.3892/mmr.2020.10927. [PubMed: 31922235]

- [28]. Li F, MacKenzie KR, Jain P, Santini C, Young DW, Matzuk MM, Metabolism of JQ1, an inhibitor of bromodomain and extra terminal bromodomain proteins, in human and mouse liver microsomes, *Biol. Reprod.* 103 (2020) 427–436. 10.1093/biolre/ioaa043. [PubMed: 32285106]
- [29]. Lewin J, Soria J-C, Stathis A, Delord J-P, Peters S, Awada A, Aftimos PG, Bekradda M, Rezai K, Zeng Z, Hussain A, Perez S, Siu LL, Massard C, Phase Ib Trial With Birabresib, a Small-Molecule Inhibitor of Bromodomain and Extraterminal Proteins, in Patients With Selected Advanced Solid Tumors, *J. Clin. Oncol.* 36 (2018) 3007–3014. 10.1200/JCO.2018.78.2292. [PubMed: 29733771]
- [30]. Li K, Crews CM, PROTACs: past, present and future, *Chem. Soc. Rev.* 51 (2022) 5214–5236. 10.1039/D2CS00193D. [PubMed: 35671157]
- [31]. Bekes M, Langley DR, Crews CM, PROTAC targeted protein degraders: the past is prologue, *Nat. Rev. Drug Discov.* 21 (2022) 181–200. 10.1038/s41573-021-00371-6. [PubMed: 35042991]
- [32]. Nemeč V, Schwalm MP, Müller S, Knapp S, PROTAC degraders as chemical probes for studying target biology and target validation, *Chem. Soc. Rev.* 51 (2022) 7971–7993. 10.1039/D2CS00478J. [PubMed: 36004812]
- [33]. Sun X, Gao H, Yang Y, He M, Wu Y, Song Y, Tong Y, Rao Y, PROTACs: great opportunities for academia and industry, *Sig. Transduct. Target Ther.* 4 (2019) 1–33. 10.1038/s41392-019-0101-6.
- [34]. Wurz RP, Dellamaggiore K, Dou H, Javier N, Lo M-C, McCarter JD, Mohl D, Sastri C, Lipford JR, Cee VJ, A “Click Chemistry Platform” for the Rapid Synthesis of Bispecific Molecules for Inducing Protein Degradation, *J. Med. Chem.* 61 (2018) 453–461. 10.1021/acs.jmedchem.6b01781. [PubMed: 28378579]
- [35]. Huang Y, Yokoe H, Kaiho-Soma A, Takahashi K, Hirasawa Y, Morita H, Ohtake F, Kanoh N, Design, Synthesis, and Evaluation of Trivalent PROTACs Having a Functionalization Site with Controlled Orientation, *Bioconjugate Chem.* 33 (2022) 142–151. 10.1021/acs.bioconjchem.1c00490.
- [36]. Ohoka N, Tsuji G, Shoda T, Fujisato T, Kurihara M, Demizu Y, Naito M, Development of Small Molecule Chimeras That Recruit AhR E3 Ligase to Target Proteins, *ACS Chem. Biol.* 14 (2019) 2822–2832. 10.1021/acscchembio.9b00704. [PubMed: 31580635]
- [37]. Henning NJ, Manford AG, Spradlin JN, Brittain SM, Zhang E, McKenna JM, Tallarico JA, Schirle M, Rape M, Nomura DK, Discovery of a Covalent FEM1B Recruiter for Targeted Protein Degradation Applications, *J. Am. Chem. Soc.* 144 (2022) 701–708. 10.1021/jacs.1c03980. [PubMed: 34994556]
- [38]. Chan K-H, Zengerle M, Testa A, Ciulli A, Impact of Target Warhead and Linkage Vector on Inducing Protein Degradation: Comparison of Bromodomain and Extra-Terminal (BET) Degraders Derived from Triazolodiazepine (JQ1) and Tetrahydroquinoline (I-BET726) BET Inhibitor Scaffolds, *J. Med. Chem.* 61 (2018) 504–513. 10.1021/acs.jmedchem.6b01912. [PubMed: 28595007]
- [39]. Min J, Mayasundari A, Keramatnia F, Jonchere B, Yang SW, Jarusiewicz J, Actis M, Das S, Young B, Slavish J, Yang L, Li Y, Fu X, Garrett SH, Yun M-K, Li Z, Nithianantham S, Chai S, Chen T, Shelat A, Lee RE, Nishiguchi G, White SW, Roussel MF, Potts PR, Fischer M, Rankovic Z, Phenyl-Glutarimides: Alternative Cereblon Binders for the Design of PROTACs, *Angew. Chem. Int. Ed.* 133 (2021) 26663–26670. 10.1002/ange.202108848.
- [40]. Winter GE, Buckley DL, Paulk J, Roberts JM, Souza A, Dhe-Paganon S, Bradner JE, Selective Target Protein Degradation via Phthalimide Conjugation, *Science.* 348 (2015) 1376–1381. 10.1126/science.aab1433. [PubMed: 25999370]
- [41]. Xue G, Wang K, Zhou D, Zhong H, Pan Z, Light-Induced Protein Degradation with Photocaged PROTACs, *J. Am. Chem. Soc.* 141 (2019) 18370–18374. 10.1021/jacs.9b06422. [PubMed: 31566962]
- [42]. Ozer HG, El-Gamal D, Powell B, Hing ZA, Blachly JS, Harrington B, Mitchell S, Grieselhuber NR, Williams K, Lai T-H, Alinari L, Baiocchi RA, Brinton L, Baskin E, Cannon M, Beaver L, Goettl VM, Lucas DM, Woyach JA, Sampath D, Lehman AM, Yu L, Zhang J, Ma Y, Zhang Y, Spevak W, Shi S, Severson P, Shellooe R, Carias H, Tsang G, Dong K, Ewing T, Marimuthu A, Tantoy C, Walters J, Sanftner L, Rezaei H, Nespi M, Matusow B, Habets G, Ibrahim P, Zhang C, Mathé EA, Bollag G, Byrd JC, Lapalombella R, BRD4 Profiling Identifies Critical Chronic Lymphocytic Leukemia Oncogenic Circuits and Reveals Sensitivity

- to PLX51107, a Novel Structurally Distinct BET Inhibitor, *Cancer Discov.* 8 (2018) 458–477. 10.1158/2159-8290.CD-17-0902. [PubMed: 29386193]
- [43]. Meanwell NA, Synopsis of Some Recent Tactical Application of Bioisosteres in Drug Design, *J. Med. Chem.* 54 (2011) 2529–2591. 10.1021/jm1013693. [PubMed: 21413808]
- [44]. Hoshi A, Sakamoto T, Takayama J, Xuan M, Okazaki M, Hartman TL, Buckheit RW, Pannecouque C, Cushman M, Systematic evaluation of methyl ester bioisosteres in the context of developing alkenyldiarylmethanes (ADAMs) as non-nucleoside reverse transcriptase inhibitors (NNRTIs) for anti-HIV-1 chemotherapy, *Bioorg. Med. Chem.* 24 (2016) 3006–3022. 10.1016/j.bmc.2016.05.010. [PubMed: 27234889]
- [45]. Ward E, DeSantis C, Robbins A, Kohler B, Jemal A, Childhood and adolescent cancer statistics, 2014, *CA Cancer J. Clin.* 64 (2014) 83–103. 10.3322/caac.21219. [PubMed: 24488779]
- [46]. Di L, Kerns E, *Drug-Like Properties: Concepts, Structure Design and Methods from ADME to Toxicity Optimization*, 2nd edition, Academic Press, Amsterdam; Boston, 2016.
- [47]. Di L, Fish PV, Mano T, Bridging solubility between drug discovery and development, *Drug Discov.* 17 (2012) 486–495. 10.1016/j.drudis.2011.11.007.
- [48]. Ottaviani G, Martel S, Carrupt P-A, Parallel Artificial Membrane Permeability Assay: A New Membrane for the Fast Prediction of Passive Human Skin Permeability, *J. Med. Chem.* 49 (2006) 3948–3954. 10.1021/jm060230+. [PubMed: 16789751]
- [49]. Lipinski CA, Lombardo F, Dominy BW, Feeney PJ, Experimental and computational approaches to estimate solubility and permeability in drug discovery and development settings, *Adv. Drug Deliv. Rev.* 64 (2012) 4–17. 10.1016/j.addr.2012.09.019.
- [50]. Bohnert T, Gan L-S, Plasma protein binding: from discovery to development, *J. Pharm. Sci.* 102 (2013) 2953–2994. 10.1002/jps.23614. [PubMed: 23798314]
- [51]. Baranczewski P, Staczak A, Sundberg K, Svensson R, Wallin A, Jansson J, Garberg P, Postlind H, Introduction to in vitro estimation of metabolic stability and drug interactions of new chemical entities in drug discovery and development, *Pharmacol. Rep.* 58 (2006) 453–472. [PubMed: 16963792]
- [52]. Pelkonen O, Turpeinen M, Raunio H, In vivo-in vitro-in silico pharmacokinetic modelling in drug development: current status and future directions, *Clin. Pharmacokinet.* 50 (2011) 483–491. 10.2165/11592400-000000000-00000. [PubMed: 21740072]

### Highlights

- A PROTAC X-ray structure inspired synthesis of JQ1-based heteroaromatic amides.
- Best derivatives showed improved overall profile compared to JQ1 and birabresib.
- X-ray structure of **SJ1461**-BRD4 complex provided a rationale for improved affinity.
- **SJ1461** is being evaluated as a potential clinical candidate.

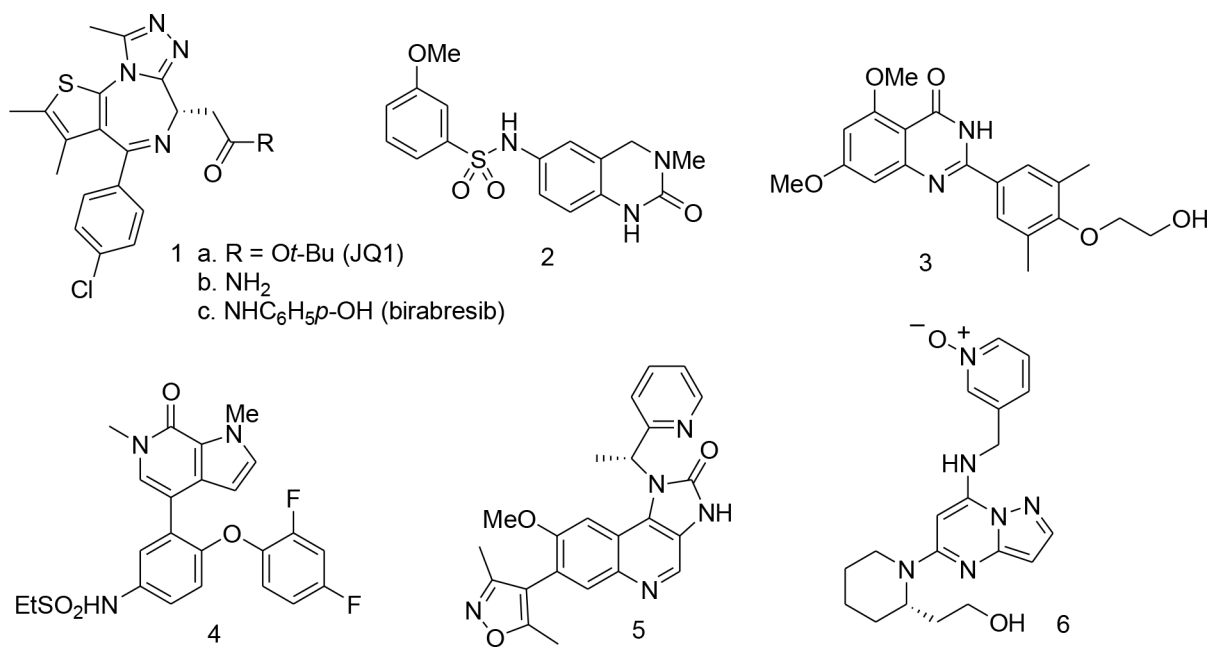


**Figure 1.**  
Selected BET inhibitors reported in the literature

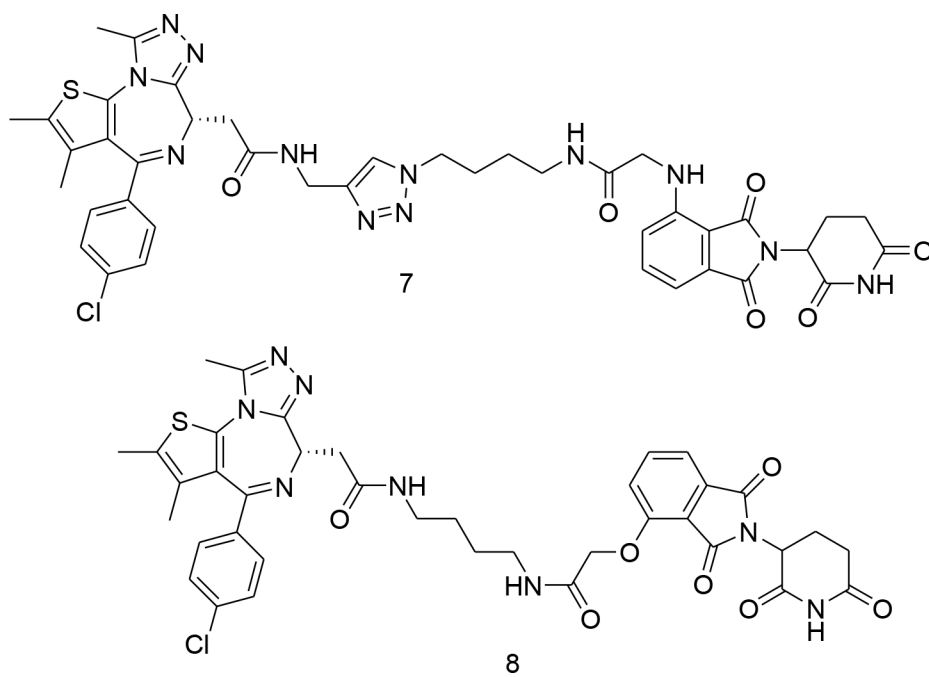


**Figure 2.**  
JQ1 derived PROTAC compounds



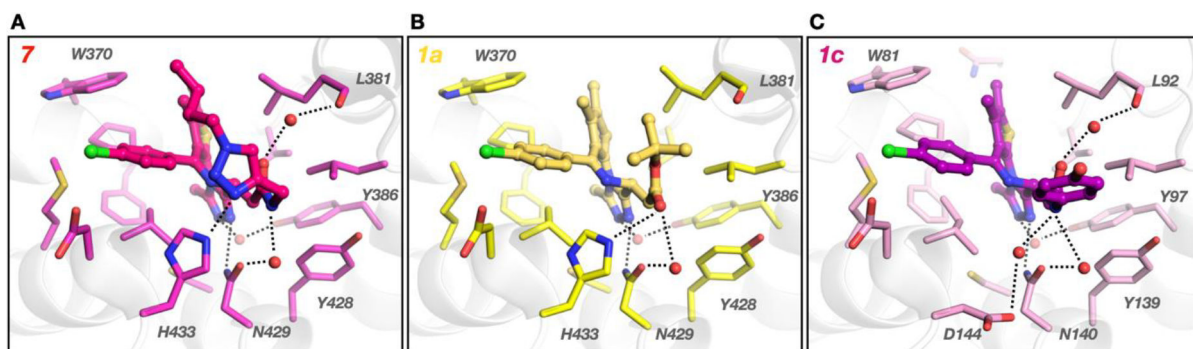


**Figure 3.**

Comparison of ligand binding modes of BET family members. Crystal structure of BRD2/BD2 in complex with (A) **7** (magenta, PDB: 6WWB) and (B) JQ1, **1a**, (yellow, PDB: 3ONI). (C) Crystal structure of birabresib, **1c**, bound to BRD4/BD1 (purple, PDB: 5WMD). Hydrogen bonds are shown as dotted lines.

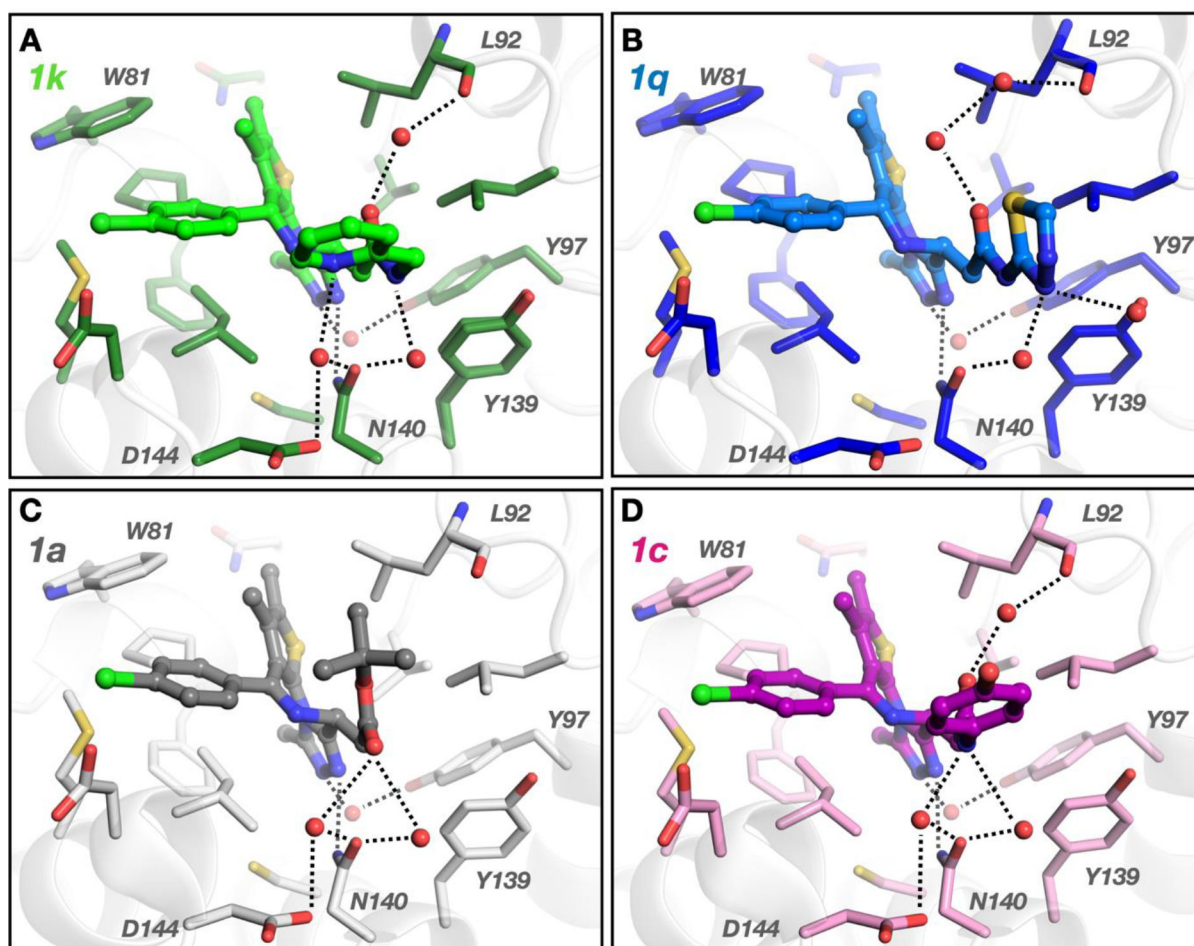
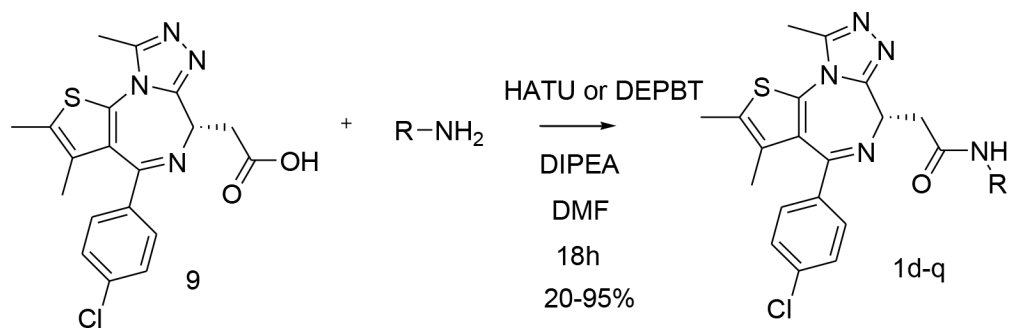


**Figure 4.**

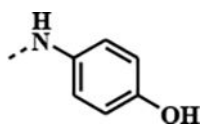
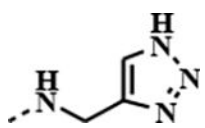
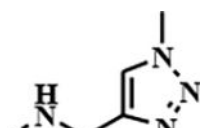
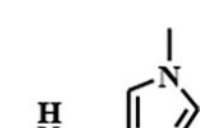
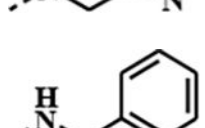
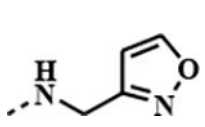
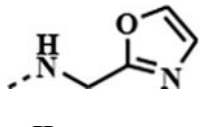
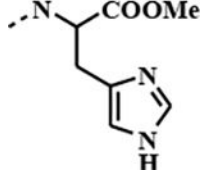
High-resolution structures of JQ1 derivatives bound to BRD4(BD1). (A) **1k** interacts with Asn140, Asp144, and Leu92 (PDB: 7RN2). (B) **1q** interacts with Asn140 and Tyr139 (PDB: 7RMD). (C) JQ1 **1a** (PDB: 3MXF) interacts with Asn140 and Asp144. (D) birabresib **1c** (PDB: 5WMD) interacts with Asn140, Asp144, and Leu92. Dotted lines represent hydrogen bonds and red spheres represent ordered water molecules. Ligand electron densities are shown in SI Fig S2.

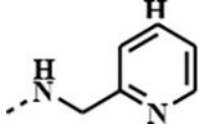
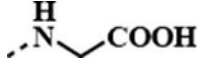
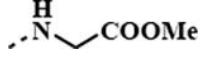
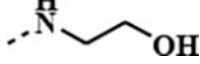
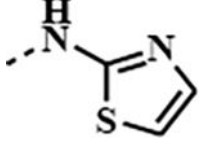
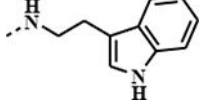
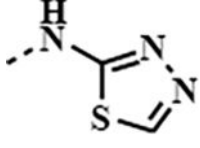


**Scheme 1.**  
Synthesis of amide derivatives

Table 1.

Potency of the JQ1 amide derivatives<sup>a</sup>

compound	1, NHR	IC <sub>50</sub> [μM] <sup>b</sup>		IC <sub>50</sub> [μM] <sup>b</sup>	
		BRD4 (BD1)	BRD4(BD2)	BRD2 (BD1)	BRD2(BD2)
1a (JQ1)	-	0.0482	0.0132	0.0285	0.0095
1c (birabresib)		0.1810	0.0098	0.0587	0.0032
1d		0.0790	0.0013	0.0086	0.0018
1e		1.4127	0.0261	0.6396	0.1616
1f		0.0823	0.0006	0.0176	0.0030
1g		0.7251	0.0003	0.0217	0.0002
1h		0.0057	0.0002	0.0031	0.0001
1i		0.0104	0.0003	0.0092	0.0001
1j		0.0346	0.0065	0.0321	0.0096

compound	1, NHR	IC <sub>50</sub> [μM] <sup>b</sup>		IC <sub>50</sub> [μM] <sup>b</sup>	
		BRD4 (BD1)	BRD4(BD2)	BRD2 (BD1)	BRD2(BD2)
1k		0.0405	0.0007	0.0163	0.0003
1l		0.1058	0.0004	0.1467	0.0003
1m		0.0028	0.0001	0.0034	0.0001
1n		0.0212	0.0033	0.0222	0.0025
1o		0.5138	0.0016	0.0109	0.0026
1p		0.7401	0.0600	0.2529	0.0505
1q (SJ1461)		0.0065	0.0002	0.0016	0.0001

<sup>a</sup>See Supporting Information for SD values.

<sup>b</sup>TR-FRET assay.

**Table 2.**Cell lines studies of the amide derivatives<sup>a</sup>

amide	HDMB03, IC50, uM	D283, IC50, uM	NALM16, IC50, uM	MOLM-13, IC50, uM	MV-4-11, IC50, uM
<b>1a</b> (JQ1)	0.0903	0.0609	0.0189	0.0247	0.099
<b>1c</b> (birabresib)	0.1343	0.0669	0.0140	0.0112	0.022
<b>1d</b>	0.0038	0.9645	0.0073	0.0035	0.253
<b>1e</b>	0.0407	0.2275	0.0145	0.0110	0.059
<b>1f</b>	0.3589	0.7892	0.0938	0.0526	0.143
<b>1g</b>	0.6190	0.5763	0.4524	0.3857	0.729
<b>1h</b>	0.0173	0.0252	0.0121	0.0147	0.032
<b>1i</b>	0.0010	0.0187	0.0008	0.0022	0.018
<b>1j</b>	1.2443	2.9340	0.7914	0.2002	1.138
<b>1k</b>	0.2630	0.2280	0.0148	0.0089	0.444
<b>1l</b>	9.3408	>8.8486	>8.8486	2.4027	3.055
<b>1m</b>	0.3592	0.3374	0.0164	0.0099	0.297
<b>1n</b>	0.0427	0.4132	0.0071	0.0088	0.033
<b>1o</b>	0.0046	0.1493	0.0064	0.0220	0.040
<b>1p</b>	0.2546	0.7492	0.1723	0.3189	0.182
<b>1q</b> (SJ1461)	0.0066	0.0562	0.0036	0.0102	0.020

<sup>a</sup>See supporting information for full data



**Table 3.**Physico-chemical and ADME properties of the JQ1 derived amides<sup>a</sup>

amide	Solubility (pH 7.4, $\mu\text{M}$ )	PAMPA <sup>b</sup> ( $10^{-6}\text{cm/s}$ )	Caco2 A/B (nm/s)	Caco2 B/A (nm/s)	Efflux Ratio	PB (%)	PS <sup>c</sup> ( $t_{1/2},\text{h}$ )	MS ( $t_{1/2},\text{h}$ )
<b>1a</b>	37.5	ULOQ	64.0	46.7	0.7	99.2	ULOQ	0.4
<b>1c</b>	23.4	315.1	221.6	485.4	2.2	97.3	ULOQ	1.7
<b>1f</b>	65.7	0.0	9.2	311.2	34.0	98.5	ULOQ	0.5
<b>1d</b>	57.4	2.1	2.5	28.0	11.2	94.8	ULOQ	0.6
<b>1g</b>	34.1	1797.1	42.2	44.5	1.1	98.7	ULOQ	0.1
<b>1e</b>	80.8	14.0	6.2	246.5	39.9	97.5	ULOQ	0.5
<b>1h</b>	56.9	274.5	150.3	777.9	5.2	93.5	ULOQ	0.4
<b>1k</b>	72.5	177.5	98.4	568.4	5.8	97.2	ULOQ	0.1
<b>1n</b>	76.1	20.8	7.0	83.3	11.9	86.9	ULOQ	3.2
<b>1m</b>	63.3	231.3	63.8	307.3	4.8	91.0	15.8	1.1
<b>1i</b>	62.0	97.2	30.4	297.4	9.8	94.1	ULOQ	5.8
<b>1o</b>	12,41	544.8	19.1	41.1	2.2	98.2	ULOQ	1.1
<b>1j</b>	68.4	0.0	7.7	14.2	1.8	92.7	24.7	4.7
<b>1l</b>	66.4	0.5	4.5	7.8	1.7	85.6	ULOQ	11.3
<b>1p</b>	1.9	ULOQ	5.7	13.8	2.4	99.6	ULOQ	0.3
<b>1q</b>	12.0	534.0	66.5	180.1	2.7	97.2	ULOQ	3.2

<sup>a</sup>See supporting information for full data; PAMPA: Parallel artificial membrane permeability assay; Caco2: human colorectal adenocarcinoma cells permeability assay; PB: human plasma binding; PS: human plasma stability; MS: metabolic stability (human microsomes).

<sup>b</sup>ULOQ on the PAMPA value indicates compound quantification was upper the limit of quantification ( $>1800 \times 10^{-6}\text{cm/s}$ ).

<sup>c</sup>ULOQ on the PS value indicates compound quantification was upper the limit of quantification ( $>100\text{ h}$ ).

**Table 4.**In vivo pharmacokinetic studies for **1q**

Route	Dose (mg/kg)	T <sub>max</sub> (h)	C <sub>0</sub> /C <sub>max</sub> (ng/mL)	AUC <sub>last</sub> (hr*ng/mL)	T <sub>1/2</sub> (hr)	CL/CL <sub>F</sub> (mL/min/kg)	V <sub>ss</sub> /V <sub>Z-F</sub> (L/kg)	F (%)
IV	1	NA	1931.3	1567.1	1.5	10.6	0.8	NA
PO	3	1.00	1555.3	3275.4	3.9	15.2	5.2	70
PO	10	0.50	3155.6	9473.0	3.9	17.5	6.0	60

T<sub>max</sub>: the time to achieve the highest concentration of drug in the blood

C<sub>max</sub>: maximal concentration of drug

AUC: area under the curve

T<sub>1/2</sub>: elimination half-life

CL: clearance

V<sub>ss</sub>: volume of distribution

F: bioavailability